

Electronic Supplementary Information

Polycyclic aromatic hydrocarbon with tetraimides as n-type semiconductor

Xiaoping Cui,^{a,c} Chengyi Xiao,^b Lei Zhang,^b Yan Li,^c and Zhaoxi Wang^{a,c}

^a Key laboratory for Advanced Materials and Institute of Fine Chemicals, East China University of Science and Technology, Meilong Road No.130,shanghai,200237,China

^b College of Energy, Beijing University of Chemical Technology, Beijing 100029, P. R. China

^c Key Laboratory of Organic Solids, Beijing National Laboratory for Molecular Sciences, Institute of Chemistry, Chinese Academy of Sciences, Beijing 100190, P. R. China

Contents

- 1. Synthesis and characterization of the compounds**
- 2. UV and CV spectra of the compounds**
- 3. Computational Methodology**
- 4. OFET Fabrication and Characterization**
- 5. NMR Spectra of the compounds**
- 6. HR-MALDI-TOF spectra of the compounds**
- 7. References**

1. Synthesis and Characterization of the compounds

General: ^1H NMR and ^{13}C NMR spectra were recorded in deuterated solvent on a Bruker ADVANCE NMR. ^1H NMR chemical shifts are reported in ppm downfield from tetramethylsilane (TMS) reference using the residual protonated solvent as an internal standard. MALDI-TOF-MS were determined on a Bruker BIFLEXIII Mass spectrometer with trithiophenes as matrix. All chemicals were purchased from commercial suppliers and used without further purification unless otherwise specified.

Synthesis of compound 3a, and 3b

A mixture of 1^[1] (0.18mmol), compound 2(0.48mmol), Pd(PPh₃)₄(0.04mmol), and CuI (0.08mmol) reflux in dry toluene(15ml) under argon for 12h, after cooling to room temperature, the solvent was concentrated in vacuo and purified by silica gel chromataphy(DCM).

3a: Yield: 73%. ^1H NMR (400 MHz, CDCl₃): 8.75(d, J = 7.6Hz, 2H), 8.66(s, 2H), 8.48(d, J = 7.6 Hz, 2H), 8.01(d, J = 8.0, 2H), 7.64(d, J = 7.6, 2H), 4.21-4.0(m, 4H), 4.04-3.92(m, 4H), 1.99-1.96(m, 2H), 1.58-1.55(m, 4H), 1.44-1.34(m, 15H), 1.25-1.18(m, 21H), 0.99-0.95(t, 6H), 0.93-0.90(t, 6H), 0.84-0.80(t, 6H); ^{13}C NMR(CDCl₃, 100MHz) : 163.92, 163.79, 162.17, 146.69, 145.10, 134.79, 134.29, 131.52, 131.28, 130.42, 129.01, 127.65, 127.07, 126.89, 125.29, 124.63, 123.73, 123.48; MALDI-TOF(m/z): calcd. for C₇₀H₇₈Br₂N₄O₈: 1263.2, found 1263.3.

3b: Yield: 64%. ^1H NMR (400 MHz, CDCl₃): 8.75 (d, J = 8 Hz, 2H), 8.66(s, 2H), 8.49 (d, J = 8 Hz, 2H), 8.01(d, J = 8 Hz, 2H), 7.63(d, J = 8 Hz, 2H), 4.21(t, 4H), 4.01-3.91(m, 4H), 1.81-1.73(m, 4H), 1.57-1.30(m, 44H), 1.23-0.91(m, 12H); ^{13}C NMR(100MHz, CDCl₃): 163.53, 163.40, 162.18, 162.13, 146.65, 145.12, 134.75, 134.27, 131.43, 131.22, 130.34, 128.97, 127.69, 127.07, 126.89, 125.31, 124.66, 123.73, 123.48. MALDI-TOF (m/z): calcd. for C₇₀H₇₈Br₂N₄O₈: 1263.2, found 1263.3.

Synthesis of 4a

Bis-(triphenylphosphine)palladium(II)dichloride(11mg, 0.0158mmol) was added to a solution of 3a (100mg, 0.079mmol) and 1,8-diazabicyclo[5.4.0]undec-7-ene (48mg, 0.316mmol) in dry dimethylacetamide (3mL) under argon. The mixture was heated to 160°C with stirring for 24h, cooled to room temperature, and diluted with methylene chloride. The mixture was washed twice with water, dried over magnesium sulfate and the solvent removed in vacuo. The crude product was purified by column chromatography (silica gel, DCM: hexane=1:2). Yield: 43%. ^1H NMR (400 MHz, CDCl₃): 8.67 (d, J = 7.2Hz, 4H), 7.85 (d, J = 7.2Hz, 4H), 4.15 (s, 4H), 2.97 (s, 4H), 1.97(s, 4H), 1.64-1.47(m, 31H), 1.11-0.67(m, 25H) ; ^{13}C NMR (100MHz, CDCl₃): 161.90, 161.56, 141.94, 134.98, 133.67, 130.99, 130.24, 125.15, 123.43, 121.29, 43.04, 42.35, 37.78, 32.00, 30.35, 29.63, 28.29, 28.26, 28.21, 27.72, 23.57, 22.93, 22.81, 14.18, 13.95, 10.10, 10.06; HR-MALDI-TOF(m/z): calcd. for C₇₀H₇₆N₄O₈: 1100.5668; Anal.Calcd for C₇₀H₇₆N₄O₈: C: 76.34%, H: 6.96%, N: 5.09%; Found: C: 75.63%, H: 6.87%, N: 5.26%..

Synthesis of 4b

Bis-(triphenylphosphine)palladium(II)dichloride(11mg, 0.0158mmol) was added to a solution of 3b (100mg, 0.079mmol) and 1,8-diazabicyclo[5.4.0]undec-7-ene(48mg, 0.316mmol) in dry dimethylacetamide (3mL) under argon. The mixture was heated to 160°C with stirring for 24h, cooled to room temperature, and diluted with methylene chloride and evaporated. The crude 4a was crystallized in toluene three times. Yield: 35%. ^1H NMR (600 MHz, CD₂Cl₂CD₂Cl₂, 80 °C): 9.05(d, J = 9Hz, 4H), 8.21 (d, J = 9 Hz, 4H), 4.34 (t, 4H), 3.70-3.66(m, 4H), 2.02-1.96(m, 4H), 1.67-1.57(m, 24H), 1.56-1.54(m, 20H), 1.52-1.41(m, 12H); ^{13}C NMR (150 MHz, CD₂Cl₂CD₂Cl₂, 80°C) : 162.13, 162.11, 142.86, 135.86, 134.41, 130.54, 126.21, 124.04, 123.91, 122.07, 42.29, 40.28, 31.88, 31.77, 29.45, 29.34, 29.24, 29.17, 28.29, 28.26, 27.52, 27.17, 22.67, 22.56, 14.06, 13.99; HR-MALDI-TOF (m/z): calcd. for C₇₀H₇₆N₄O₈: 1100.5663, found 1100.5641; Anal.Calcd for C₇₀H₇₆N₄O₈: C: 76.34%, H: 6.96%, N: 5.09%; Found: C: 75.86%, H: 6.89%, N: 5.04%.

2. UV and CV spectra of the compounds

Cyclic voltammograms (CVs) were recorded on a 1000B model electrochemical workstation using glassy carbon discs as the working electrode, Pt wire as the counter electrode, Ag/Ag⁺ electrode as the reference electrode, and ferrocene/ferrocenium as an internal potential marker. 0.1 M tetrabutylammonium hexafluorophosphate (TBAPF₆) dissolved in dichloromethane was employed as the supporting electrolyte.

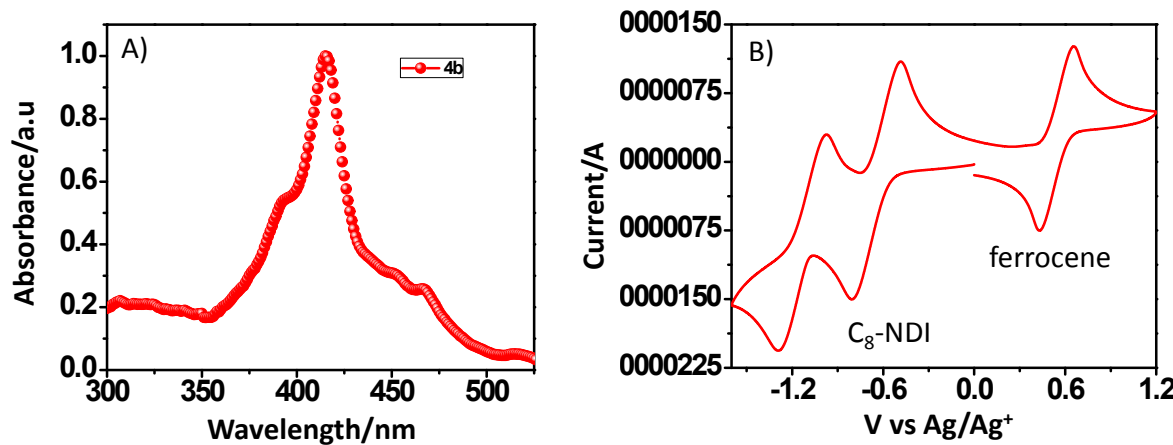


Figure S1. A) UV-vis spectra of **4b** in dichloromethane, and B) CV spectra of C₈-NDI and ferrocene in dichloromethane.

3. Computational Methodology

MO calculations were carried out with the DFT method at the B3LYP/6-31g(d) level using Gaussian 03 program package. [2]

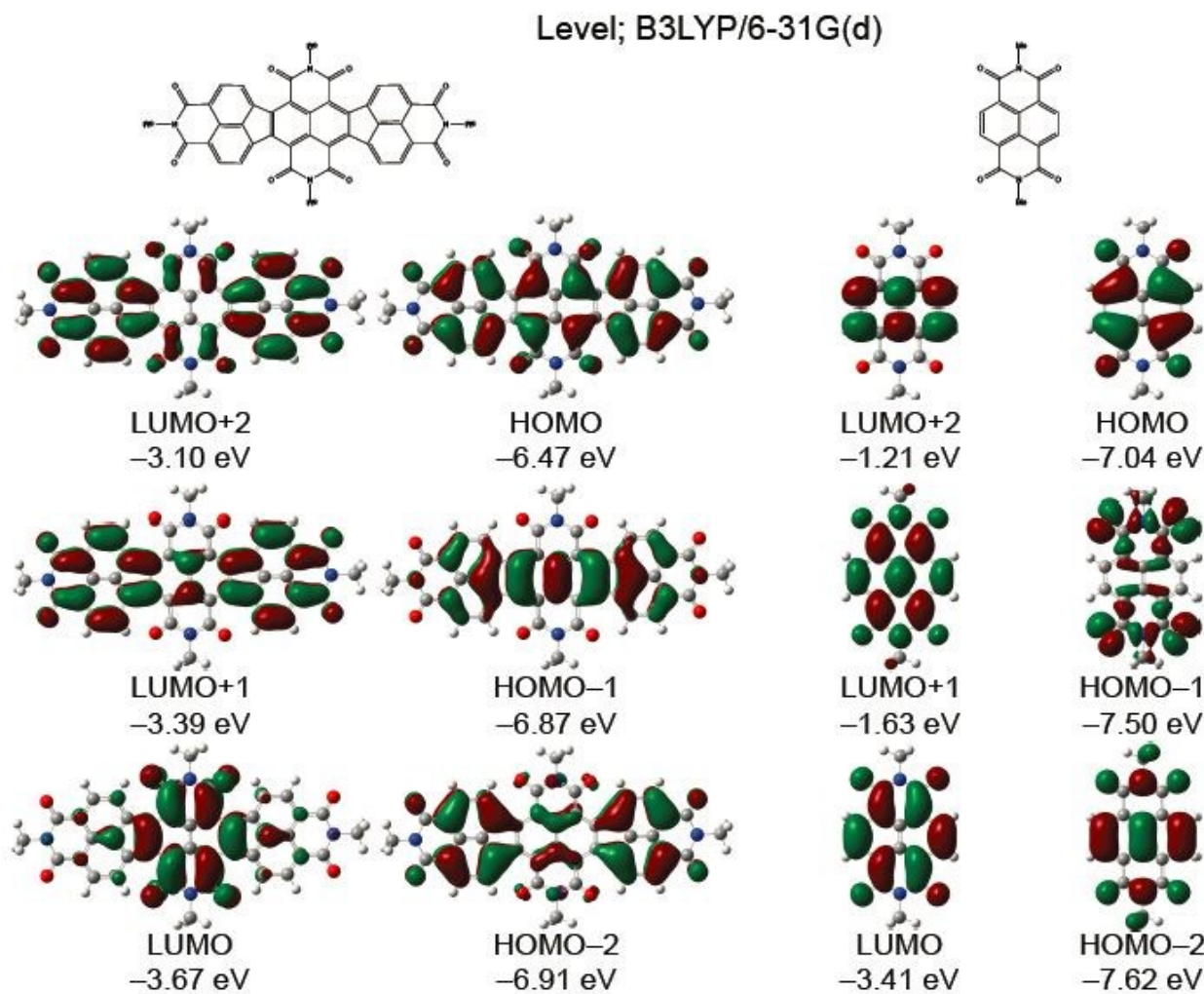


Figure S2. Calculated HOMO and LUMO of C₈-NDI, and **4a** with methyl groups instead of octyl or ethylhexyl (B3LYP/6-31g(d) level).

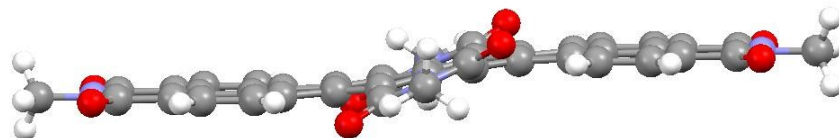


Figure S3. Optimized structure of **4a** with methyl groups instead of ethylhexyl by DFT.

4. OFET Fabrication and Characterization

The micro-/nanocrystals of **4a** and **4b** were prepared by a facile in-situ drop-coating method, where the compounds were dissolved in the dilute chloroform solution (0.5 mg/ml). The solutions were dropped onto OTS-treated (octadecyltrichlorosilane) SiO₂/Si substrates and the micro-/nanocrystals can be easily obtained with the solutions evaporated. The electrodes were made by an “gold strips” technique according to the literature.^[3]

The thin-film FET devices were fabricated in the bottom-gate, top-contact (BGTC) geometry configuration. Thin films were made by spin-coating 10 mg/ml solution of **4a**, and **4b** in chloroform on OTS-SiO₂/Si and then annealed at 150 or 200 °C for 30 mins in vacuum drying oven. Gold was deposited as source/drain electrodes using the shadow mask.

FET characteristics were obtained at room temperature in air on a Keithley 4200 SCS and Micromanipulator 6150 probe station. The mobility of the devices were calculated in the saturation regime. The equation is listed as follows:

$$I_{DS} = (W/2L)C_i\mu(V_{GS}-V_T)^2$$

where W/L (~200μm/25μm for thin film FETs) is the channel width/length , C_i is the insulator capacitance per unit area, and V_{GS} and V_T are the gate voltage and threshold voltage, respectively.

The microscope images of all the aligned microcrystal arrays were acquired by an optical microscope (Vision Engineering Co., UK), which was coupled to a CCD camera. Atomic force microscopy (AFM) measurements were carried out with a Nanoscope IIIa instrument (Digital Instruments). X-ray diffraction (XRD) was measured on a D/max2500 with a CuKα source ($\kappa = 1.541 \text{ \AA}$). SEM images were obtained with a Hitachi S-4300 microscope (Japan).

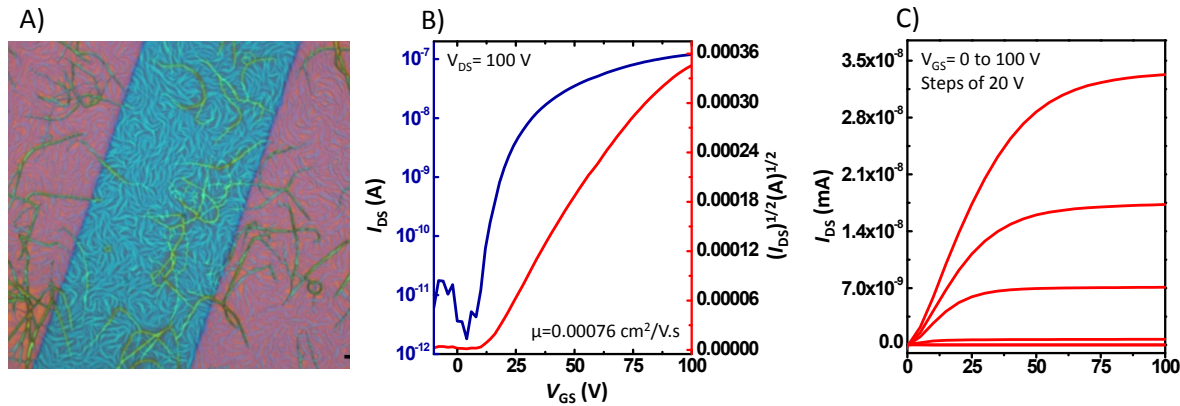


Figure S4. A) OM image of the thin-film of **4b**, B) The transfer and C) Output characteristics of OFET devices based on thin-film of **4b**.

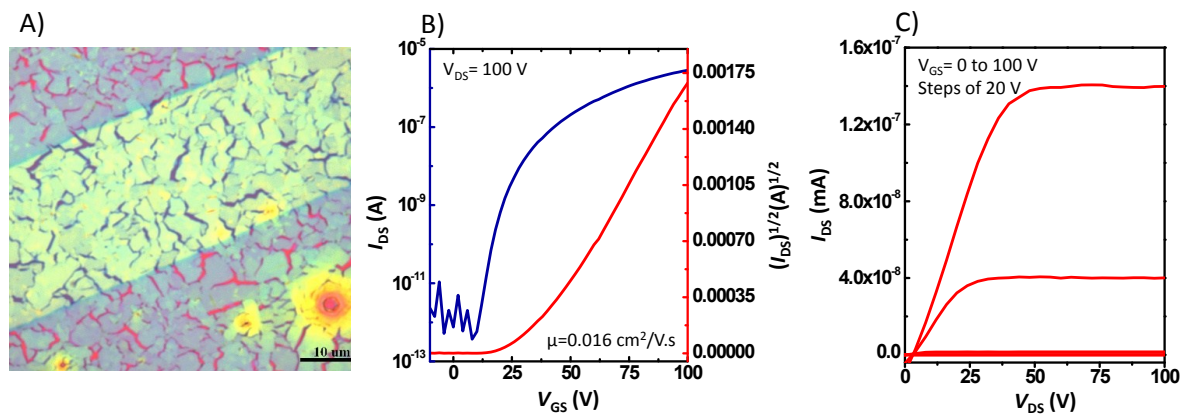


Figure S5. A) OM image of the thin-film of **4a**, B) The transfer and C) Output characteristics of OFET devices based on thin-film of **4a**.

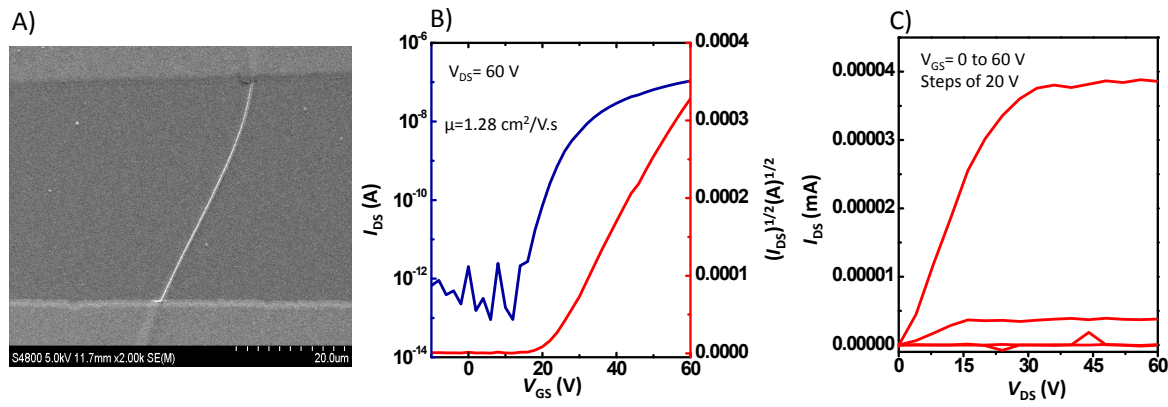


Figure S6. A) SEM image of the single-crystalline fiber of **4b** with electrodes, B) The transfer and C) Output characteristics of OFET devices based on single-crystalline fibers of **4b** (measured under ambient conditions).

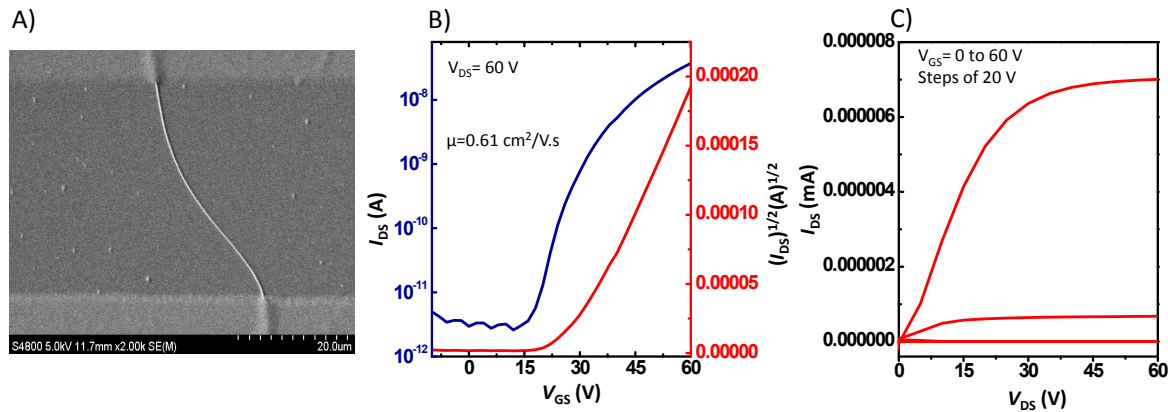


Figure S7. A) SEM image of the single-crystalline fiber of **4a** with electrodes, B) The transfer and C) Output characteristics of OFET devices based on single-crystalline fibers of **4a** (measured under ambient conditions).

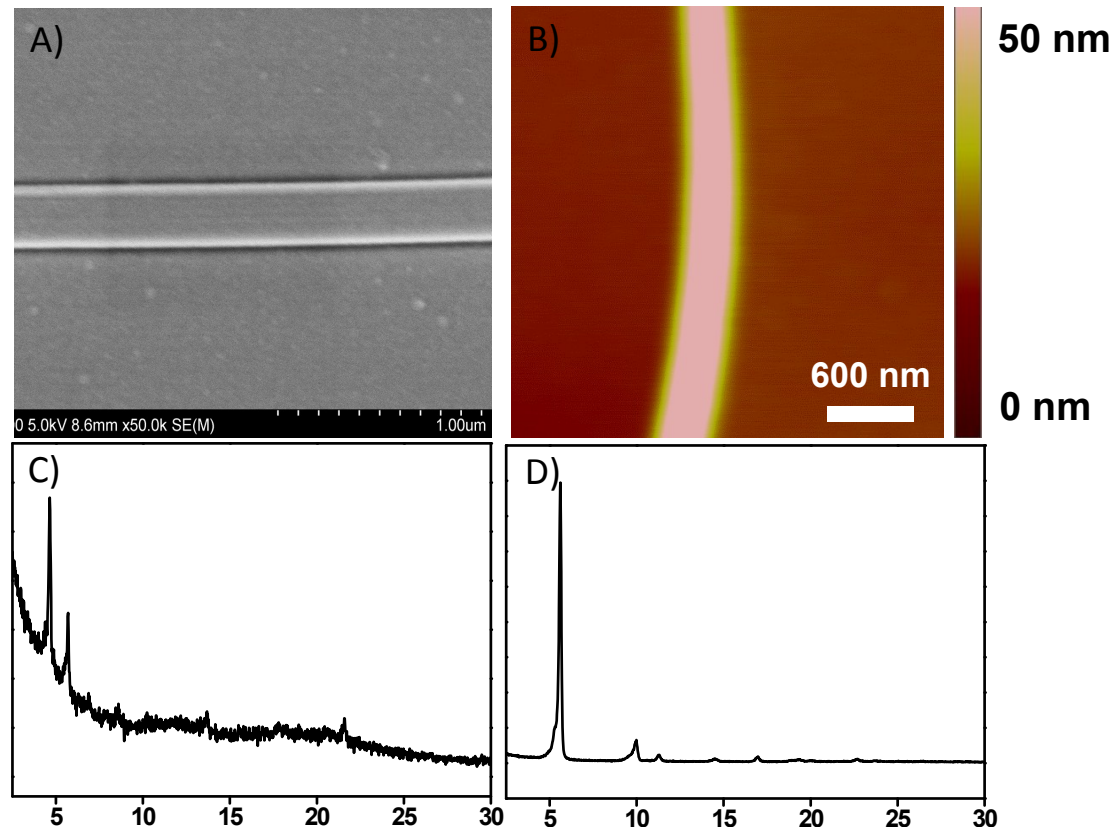


Figure S8. A) SEM image and B) AFM of the single-crystalline fiber of **4b**, C) XRD of single-crystalline fibers of **4b**, D) XRD of single-crystalline fibers of **4a**.

Table 1. The carrier mobilities of **4a** and **4b** fibers.

Compounds	Atmosphere	Mobility ^{max} /cm ² V ⁻¹ s ⁻¹	On/off Ratio
4b	Air	1.55 (1.28±0.14)^a	10⁵-10⁶
	Nitrogen	1.75 (1.50±0.15)^a	10⁵-10⁶
4a	Air	0.61 (0.46±0.09)^a	10⁵-10⁶

^a Averaged values from 10 FET devices

5. NMR Spectra of the compounds

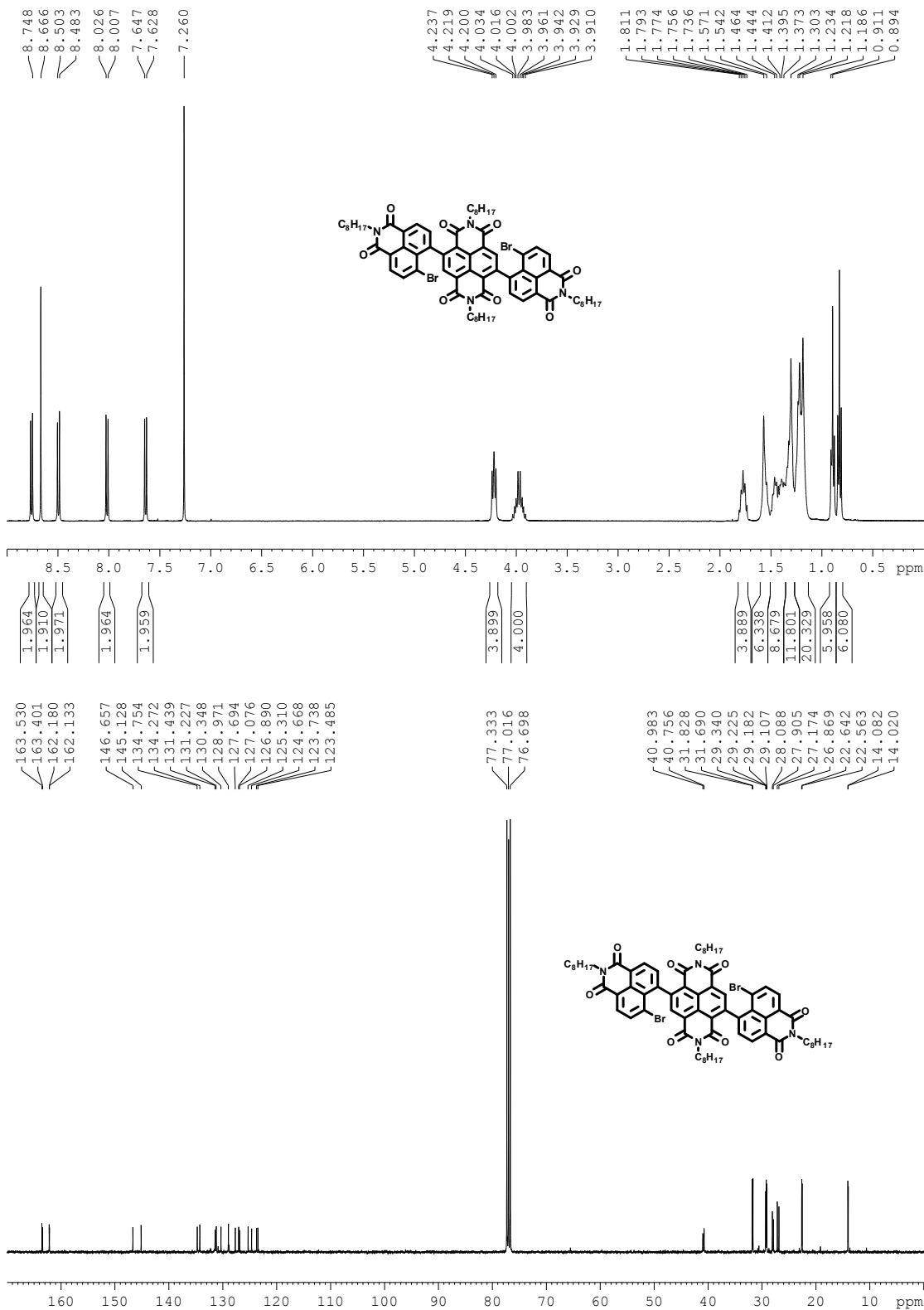


Figure S9. ^1H NMR and ^{13}C NMR of **3b**.

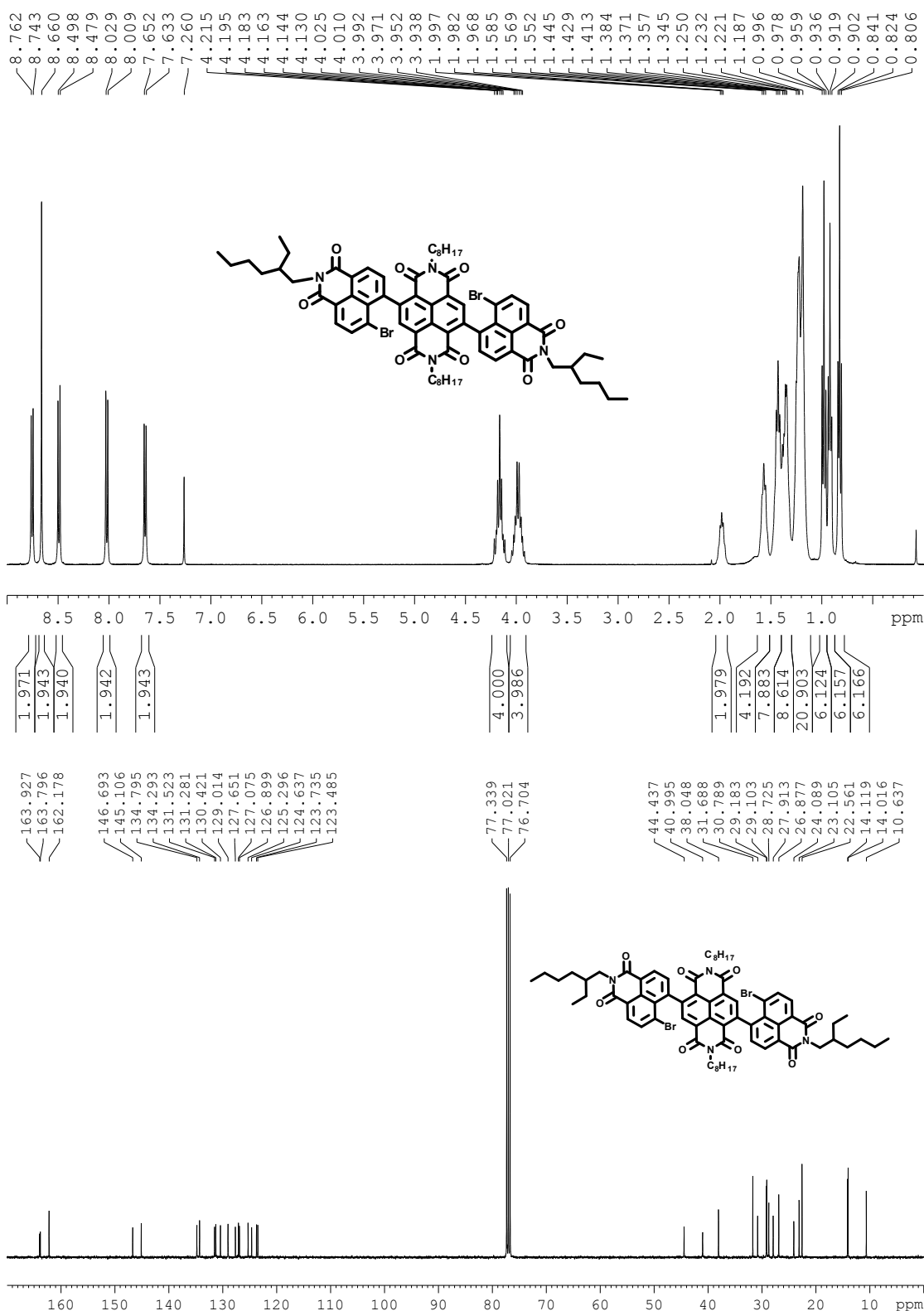


Figure S10. ^1H NMR and ^{13}C NMR of **3a**.

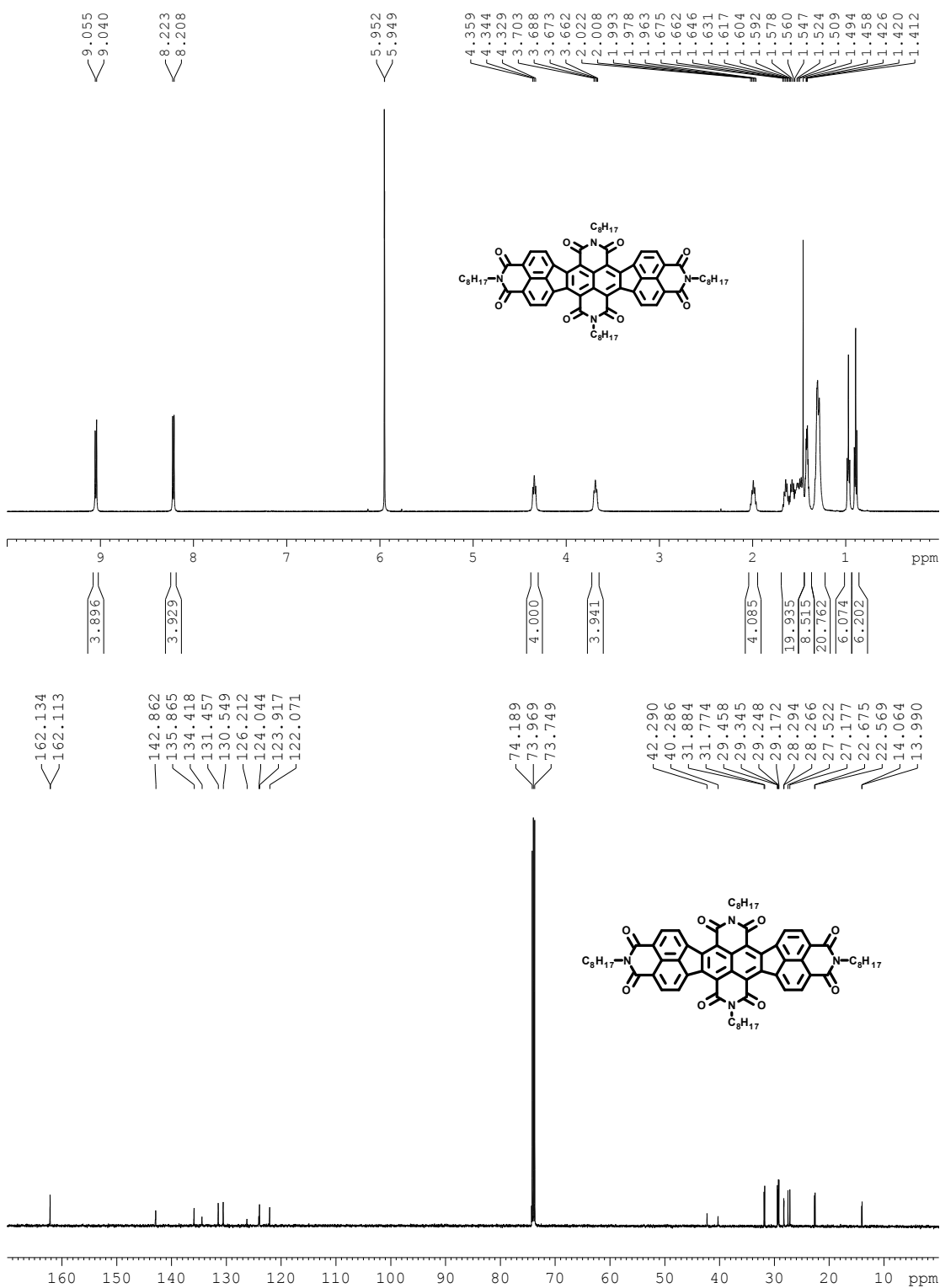


Figure S11. ¹H NMR and ¹³C NMR of **4b**.

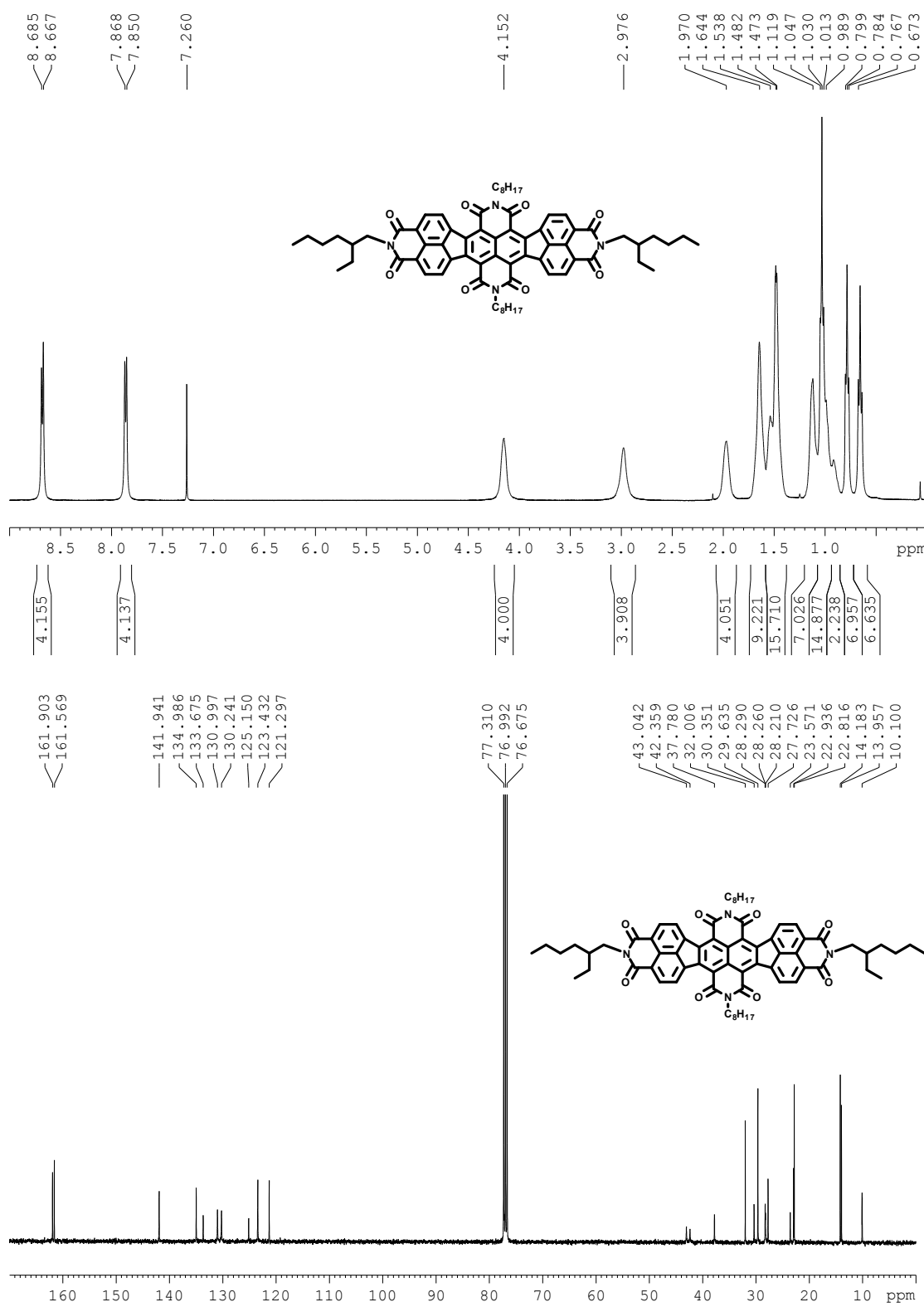


Figure S12. ^1H NMR and ^{13}C NMR of **4a**.

6. HR-MALDI-TOF spectra of the compounds

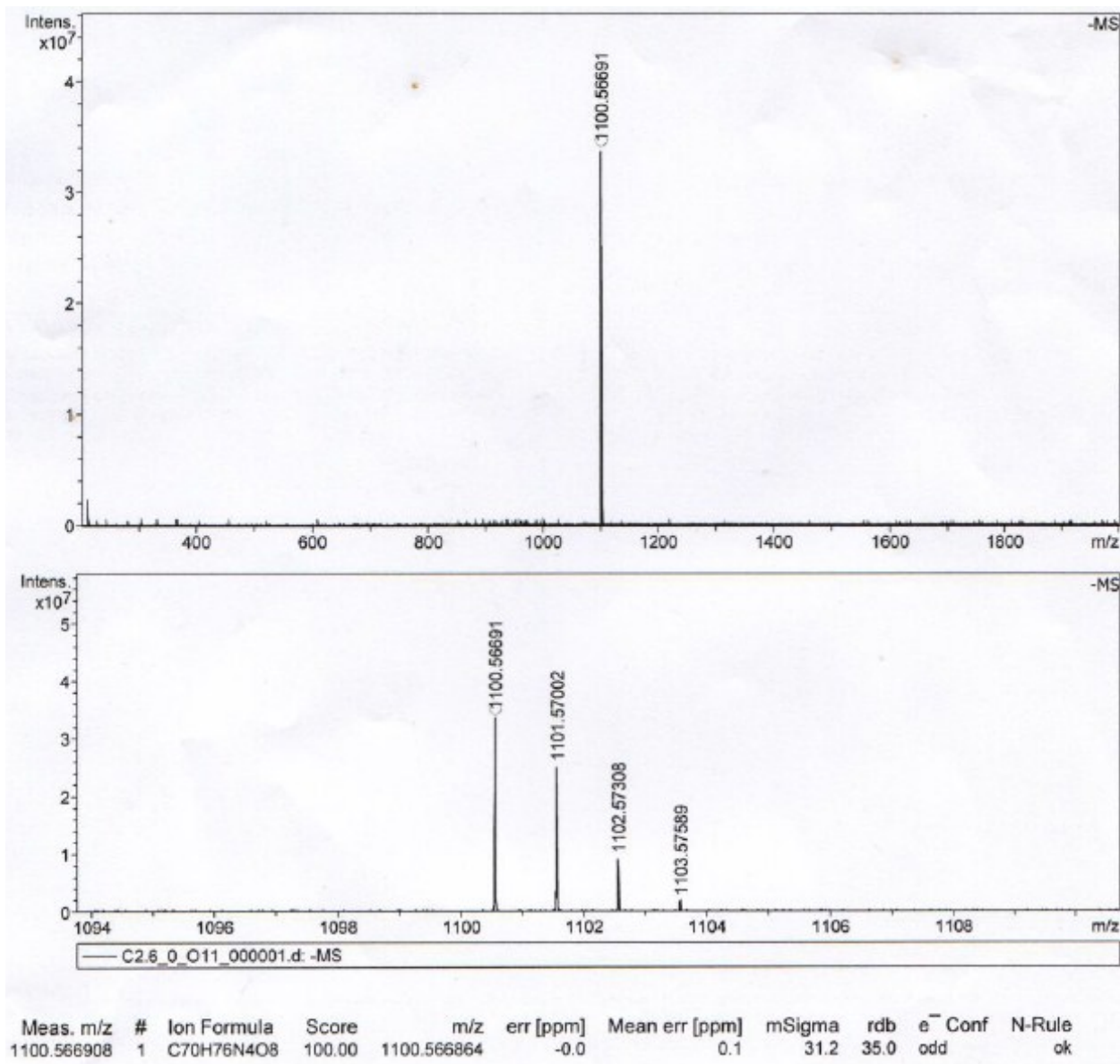


Figure S13. HR-MALDI-TOF spectra of **4b**.

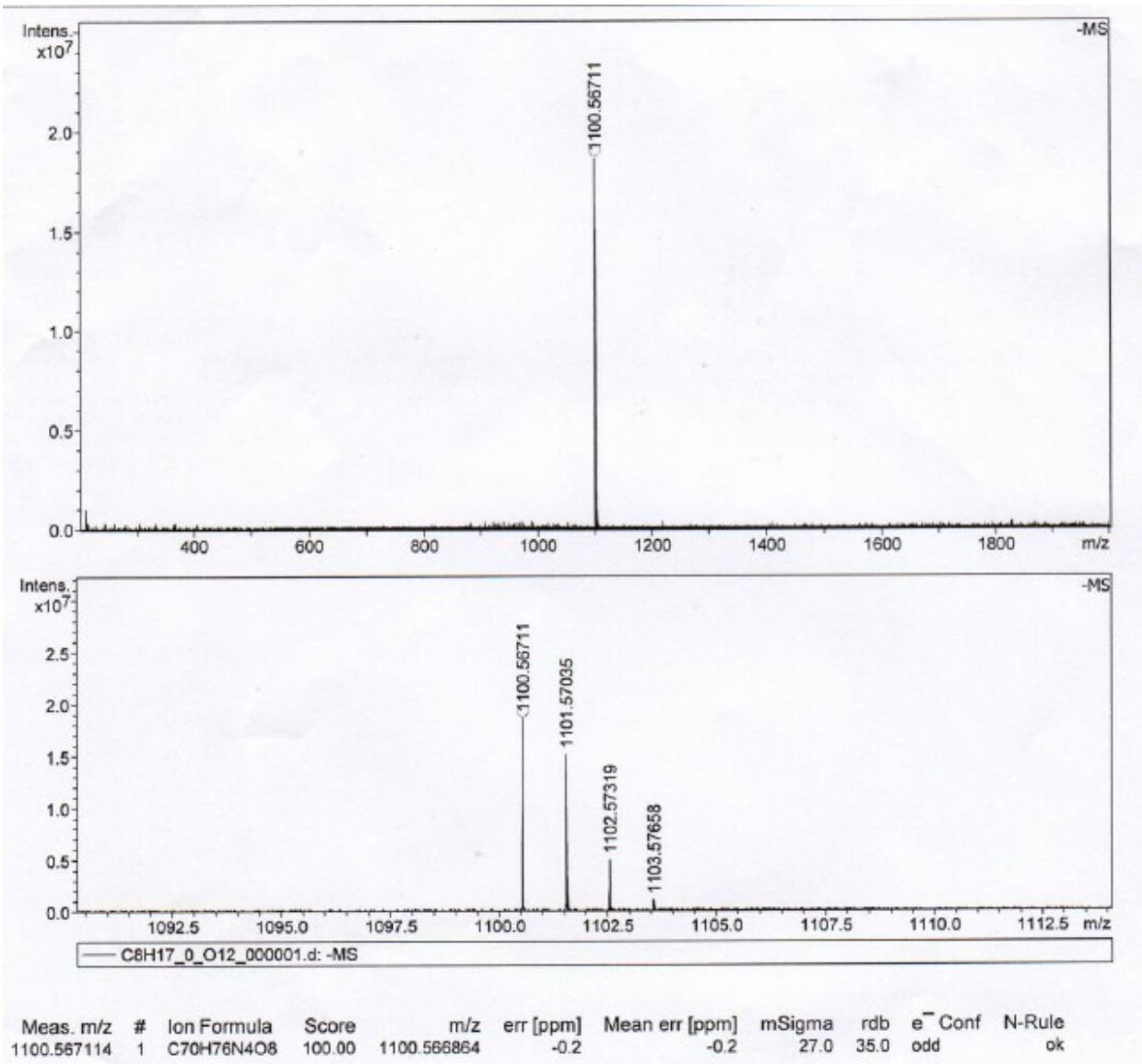


Figure S14. HR-MALDI-TOF spectra of **4a**.

7. References

- [1]. Polander, L. E.; Romanov, A. S.; Barlow, S.; Hwang, D. K.; Kippelen, B.; Timofeeva, T. V.; Marder, S. R. *Org. Lett.*, **2012**, *14*, 918.
- [2]. Frisch, M. J.; Trucks, G. W.; Schlegel, H. B.; Scuseria, G. E.; Robb, M. A.; Cheeseman, J. R.; Montgomery, Jr. J. A.; Vreven, T.; Kudin, K. N.; Burant, J. C.; Millam, J. M.; Iyengar, S. S.; Tomasi, J.; Barone, V.; Mennucci, B.; Cossi, M.; Scalmani, G.; Rega, N.; Petersson, G. A.; Nakatsuji, H.; Hada, M.; Ehara, M.; Toyota, K.; Fukuda, R.; Hasegawa, J.; Ishida, M.; Nakajima, T.; Honda, Y.; Kitao, O.; Nakai, H.; Klene, M.; Li, X.; Knox, J. E.; Hratchian, H. P.; Cross, J. B.; Adamo, C.; Jaramillo, J.; Gomperts, R.; Stratmann, R. E.; Yazyev, O.; Austin, A. J.; Cammi, R.; Pomelli, C.; Ochterski, J. W.; Ayala, P. Y.; Morokuma, K.; Voth, G. A.; Salvador, P.; Dannenberg, J. J.; Zakrzewski, V. G.; Dapprich, S.; Daniels, A.D.; Strain, M. C.; Farkas, O.; Malick, D. K.; Rabuck, A. D.; Raghavachari, K.; Foresman, J. B.; Ortiz, J.V.; Cui, Q.; Baboul, A. G.; Clifford, S.; Cioslowski, J.; Stefanov, B. B.; Liu, G.; Liashenko, A.; Piskorz, P.; Komaromi, I.; Martin, R. L.; Fox, D. J.; Keith, T.; Al-Laham, M. A.; Peng, C. Y.; Nanayakkara, A.; Challacombe, M.; Gill, P. M. W.; Johnson, B.; Chen, W.; Wong, M. W.; Gonzalez, C.; Pople, J. A.; "Gaussian 03, Revision C.02", Gaussian, Inc., Wallingford, CT, 2004.
- [3]. Lv, A.; Puniredd, S. R.; Zhang, J.; Li, Z.; Zhu, H.; Jiang, W.; Dong, H.; Hu, Y.; Jiang, L.; Li, Y.; Pisula, W.; Hu, W.; Wang, Z. *Adv. Mater.*, **2012**, *24*, 2626.